2P2-6

Stable modeling of free boundaries of an anisotropic Lamé resonator in the finite difference time domain method using Lebedev grid

Koji Hasegawa* and Ryo Kawagoe‡
(Grad. School Eng., Muroran Institute of Technology)

1. Introduction

The finite-difference time-domain (FDTD) method has simple schemes for approximating space and time derivatives of fields with discretized field values at grid points. For analysis of elastic waves propagating in solids by the FDTD method, we choose the grids from standard staggered grids (SSG),[1] Lebedev grids (LG),[2-4] rotated staggered grids (RSG),[5] or staggered grids with the collocated grid points of velocities (SGCV).[6-8] In FDTD analysis with SSG, RSG and SGCV for anisotropic media, interpolations of the velocity and stress component values off the grid points are required in general. However, in the LG, without these interpolations the FDTD scheme runs because velocity-vector and stress component gird points are at the center and four vertices of an LG cell and the centers of four LG cell edges, respectively. FDTD analyses of elastic wave propagation in isotropic and anisotropic infinite media have demonstrated validity and usefulness of the LG. In addition, a source distribution issue of a point source was overcome. [3,4] However, the stability of the LG models with free boundaries have not been examined.

In this paper, we presented a stable LG and SSG models of free boundaries in two dimensions. The stability and validity of these models were demonstrated by computing resonant frequencies of a Lamé resonator on a quartz plate in the finite-difference frequency-domain (FDFD) method for elastic waves with ignoring piezoelectricity of quartz. In addition, we show that the LG model in this FDFD analysis gives degenerate eigenvalues.

2. Stable LG Models of Free Boundaries

We consider a Lamé resonator on a quartz plate with Euler angles $(0, -29.347°, 0)$ and side length along *x* and *y* axes of l_x and $l_y = 0.9673 l_x$ on *x*-*y* plane in vacuum in two dimensions $(\partial/\partial z = 0)$. [7,8] Here, we used the Bechmann's constants and ignored the piezoelectricity. The frequency of the fundamental Lamé-mode f_0 is approximately $2411.842 / l_x$ [Hz] and the components of the stiffness being zero are $C_{i5} = C_{5i} = C_{i6} = C_{6i} = 0$ (i =1, 2, 3, 4).

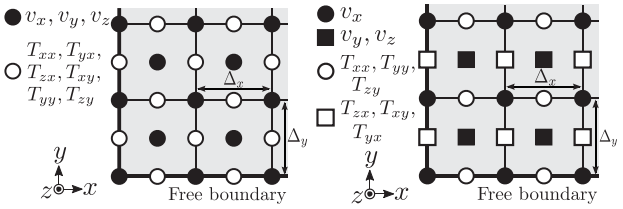

(a) LG (b) SSG

Fig. 1 Stable SSG and LG models of free boundaries.

Figure 1 shows stable SSG and LG models of free boundaries. We can compute velocities (●), and stress components (○, □) in the free boundaries by the stress imaging technique and the stress free conditions, respectively.[7,8] For a stable SSG model, a rearranged SSG is developed: v_y and v_z grid points are collocated on the same grid points for avoiding the interpolations off grid points because an SSG model in two dimensions that is a projection of the SSG in three-dimensional space, which has three staggered control volumes for each velocity component in the *x*, y, and *z*-axes, onto the *x*-*y* plane are not stable[8]. We can see that two staggered SSG models compose an LG model. Therefore, we expect that a point source in an LG model excites elastic fields in one of staggered SSG models in the FDTD analysis. In FDFD analysis, LG model yields degenerate modes.

3. Stability Analysis of FDTD Models

We used von Neumann stability analysis of FDTD models: applying central difference approximation with the second order accuracy to the spatial derivatives in Newton's translational equation of motion and the strain-displacement relation with the elastic constitutive equation, we have an equation:

$$\frac{\partial}{\partial t} f^{(n)} = \frac{R}{\Delta_t} A f^{(n)} \qquad (3)$$

where $R = V_N \Delta_t / \Delta_x$ is the Courant number, t, $f^{(n)} = \left[v^{(n)T} \; T^{(n)T} \right]^T$, A, and Δ_t are time, a field

E-mail: ‡ 20043015@mmm.muroran-it.ac.jp,
*khasegaw@mmm.muroran-it.ac.jp

column vector composed of two column vectors, velocity column vector $v^{(n)}$ and stress-tensor column vector $T^{(n)}$ with discretized field values at all grid points, the normalized matrix of finite difference spatial operator, and a time interval. Here, the superscript (n) and T denote the values at the time $t = n\Delta_t$ and transpose of the column vector. We used $V_N = (C_N/\rho)^{1/2}$ with C_N being the maximum value of the stiffness components.

Assuming that the elastic fields are time-harmonic fields with angular frequency ω, we have $f^{(n)} = f_\omega e^{j\omega n\Delta_t}$. Hence, we can derive an eigenvalue problem from (3) as follows:

$$j\frac{\omega\Delta_t}{R} f_\omega = A f_\omega \qquad (4)$$

where $(j\omega\Delta_t/R)$ and f_ω are the eigenvalue and the eigenvector of the matrix A.

Using the second order approximation of the time derivative in (3), $\partial f^{(n)}/\partial t \approx (f^{(n+1/2)} - f^{(n-1/2)})/\Delta_t = j\omega f^{(n)}$, we have a quadratic equation for $q = \exp(j\omega\Delta_t/2)$: $q^2 - (j\omega\Delta_t)q - 1 = 0$. The solutions of this equation are:

$$q = j\omega\Delta_t/2 \pm \left[1 + \left(j\omega\Delta_t/2\right)^2\right]^{1/2}. \qquad (5)$$

If $|q| \le 1$, FDTD fields are stable.

Hence, the FDTD model is stable when all computed eigenvalues $(j\omega\Delta_t/R)$ of A in (4) are $\mathrm{Re}(j\omega\Delta_t/R) = 0$ and $|\mathrm{Im}(j\omega\Delta_t/R)| \le 2/R$.

4. Numerical Results

We divide the resonator into $N \times N$ unit cells or rectangular elements whose sides have identical length, Δ_x and Δ_y, where $N = l_x/\Delta_x = l_y/\Delta_y$.

Figure 2 shows distributions of eigenvalues of (4) by the FDFD method with $N = 2^6$. The maxima of real parts of eigenvalues, $\max|\mathrm{Re}(j\omega\Delta_t/R)|$, with LG and SSG models are smaller than 10^{-9} and 2×10^{-13}, and $\max|\mathrm{Im}(j\omega\Delta_t/R)|$ is the same value of 2.84434. Hence, we may conclude that two FDTD models are stable.

Table 1 shows the computed results $\hat{f}l_x$ for the lowest five modes. The SSG result and one of the LG results are the same in six digits for the lowest five modes. Their field distributions at the grid points belong to the SSG model are also the same and the distributions at other grid points of the LG models have sufficiently small amplitude to identify as a distribution on another SSG model. Hence, we can confirm that the presented LG model is composed of staggered SSG models and the mode field independently exists in each SSG model.

Figure 3 shows dependence of $\widehat{f_0}l_x$ on the value of N where $\widehat{f_0}$ is computed result of f_0. We also presented FDFD results with SGCV models[8] and FEM results with linear rectangular elements (four nodes) and serendipity rectangular elements (eight nodes). We can see that computed results of LG and SSG are the same values, errors of four node FEM analysis almost equal to SGCV results at the same N, and the errors are larger than the LG results.

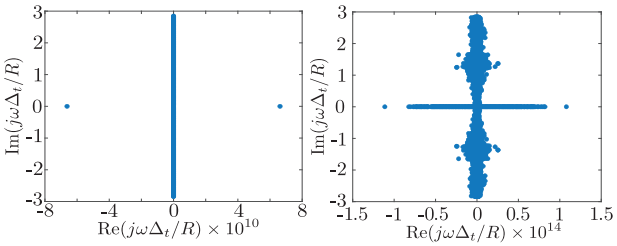

(a) LG (b) SSG

Fig.2 Eigenvalue distributions computed by FDFD method with LG and improved SSG models.

Table 1 Computed results of $\hat{f}l_x$.

$\hat{f}l_x$ [m/s]				
FEM		LG	SSG	SGCV
4 nodes	8 nodes			
2412.42	2411.84	2411.60 2411.60	2411.60	2412.60
2383.95	2383.30	2383.27 2382.50	2382.50	2383.61
2325.79	2325.06	2325.02 2324.16	2325.02	2325.38
2251.74	2251.50	2251.28 2251.27	2251.27	2251.32
1724.92	1724.73	1724.57 1724.54	1724.54	1724.57

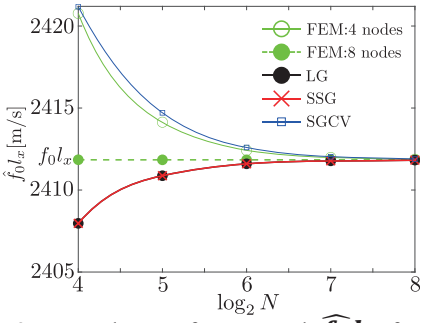

Fig.3 Dependence of computed $\widehat{f_0}l_x$ for the fundamental Lamé mode, on the number of divisions N.

References

1) J. Virieux, Geophysics **51**, 889 (1986).
2) V. I. Lebedev, USSR Comput. Math. Math. Phys. **4**, 69 (1964).
3) V. Dmitry, L. Vadim, T. Vladimir, and R. Galina, Geophysics **79**, T219 (2014).
4) E. F. M. Koene, J. O. A. Robertsson, and F. Andersson, Geophysics **86**, A21(2021).
5) E. H. Saenger, N. Gold, and S. A. Shapiro, Wave Motion **31**, 77 (2000).
6) K. Hasegawa and T. Shimada, Jpn. J. Appl. Phys. **51**, 07GB04 (2012).
7) A. Koda and K. Hasegawa, Proc. 41st Symp. on Ultrasonic Electronics, 2020, 2Pa1-2.
8) K. Hasegawa and R. Kano, Proc. 43rd Symp. on Ultrasonic Electronics, 2022, 1Pb2-6.